Oxygenation of offshore Southern California Marine Basins through the Holocene

Hannah M. Palmer[1,2], Tessa M. Hill[1,2], Esther G. Kennedy[1,2], Peter D. Roopnarine[3], Sonali Langlois[4], Katherine R. Reyes[5], and Lowell D. Stott[6]

1. Earth and Planetary Sciences, University of California, Davis
2. Bodega Marine Laboratory, University of California, Davis
3. California Academy of Sciences
4. Santa Rosa Junior College
5. Dominican University of California
6. University of Southern California

Corresponding author: Hannah M. Palmer (hmpalmer@ucdavis.edu)

Key Points:

- In the Southern California Borderlands, oxygenation below 1400 m was stable and reduced relative to modern from 11.2-4.7 ka.
- San Nicolas Basin experienced an oxygenation episode from 4.7-4.2 ka and oxygenation increased in Tanner Basin gradually from 5.5-1.9 ka.
- Variance in reconstructed Holocene dissolved oxygen concentration is similar to decadal scale variance in modern dissolved oxygen

Abstract

In the face of ongoing marine deoxygenation, understanding timescales and drivers of past oxygenation change is of critical importance. Marine sediment cores from tiered silled basins provide a natural laboratory to constrain timing and implications of oxygenation changes across multiple depths. Here, we reconstruct oxygenation change over time using benthic foraminiferal assemblages from three sediment cores, EW9504-09PC (Tanner Basin, 1194 m water depth), EW9504-08PC (San Nicolas Basin, 1442 m), and EW9504-05PC (San Clemente Basin, 1818 m) across the Southern California Borderlands. We utilize indicator taxa, community ecology, and an oxygenation transfer function to reconstruct past oxygenation, and directly compare reconstructed dissolved oxygen to modern measured dissolved oxygen. We generate new, higher resolution carbon and oxygen isotope records from planktic (*Globigerina bulloides*) and benthic foraminifera (*Cibicides mckannai*) from Tanner Basin. Early to mid-Holocene (11.2-4.7 ka) oxygenation below 1400 m (San Clemente and San Nicolas Basins) was relatively stable and reduced relative to modern. San Nicolas Basin experienced a multi-centennial oxygenation episode from 4.7-4.2 ka and oxygenation increased in Tanner Basin gradually from 5.5-1.9 ka. Oxygenation of these offshore basins is synchronous with an increase in oxygenation in Santa Barbara Basin at ~6 ka and may be due to increased oxygenation of North Pacific Intermediate Water. Yet across all three depths and time intervals studied, dissolved oxygen is consistently within a range of intermediate hypoxia (0.5-1.5 ml L^{-1} O_2). Variance in reconstructed dissolved oxygen was similar to decadal variance in modern dissolved oxygen and reduced relative to Holocene-scale changes in shallower basins.

Plain Language Summary

Globally, marine oxygenation is declining with detrimental impacts to ecosystems and economies. To better understand the drivers and consequences of ocean oxygen change, we can examine the fossil record to identify how oxygenation changed in the past. Specifically, we use the relative abundance and chemistry of microfossils (i.e., foraminifera) to reconstruct past oxygenation. Here, we examined microfossils from three sediment cores in three basins (Tanner, San Nicolas, San Clemente) off the coast of Southern California. Oxygenation below 1400 m water depth was relatively stable and lower than to modern from 11,200 to 4,200 years before present. San Nicolas Basin experienced a multi-centennial oxygenation episode from 4,700-4,200 years before present and oxygenation increased in Tanner Basin gradually from 5,500-1,900 years before present. This may have been caused by low-oxygen water being transported to the basins from the North Pacific. When compared to modern, the range of values of reconstructed oxygen through the entire time studied (thousands of years) is similar to the range of values of modern oxygen at the same depths, indicating that the changes in the last ten thousand years were similar to the amount of change occurring on annual and decadal timescales in the modern ocean.

1 Introduction

1.1 Marine oxygenation in the past and present

At present, global marine oxygenation is declining due to anthropogenic climate change, with important implications for benthic and pelagic ecosystems (Breitburg et al., 2018; Oschlies et al., 2018; Schmidtko et al., 2017, 2017). Ocean oxygenation, particularly at depth, is an important driver of ecosystem zonation, and expansion of oxygen minimum zones (OMZ) is a current threat to global marine ecosystems (Breitburg et al., 2018; Helly & Levin, 2004; Stramma, Schmidtko, et al., 2010). Deoxygenation at depth can be driven by several processes: increased export of organic matter from surface to depth leading to increased respiration below the photic zone, increased stratification (often due to surface warming) reducing ventilation at depth, warming surface temperatures reducing rates of diffusion of atmospheric oxygen into surface waters, and changes in the source, current velocity, or oxygenation of intermediate waters (Levin et al., 2009; Oschlies et al., 2018; Stramma, Schmidtko, et al., 2010).

Understanding drivers and timescales of changes to marine oxygenation is critical for understanding and predicting future change (Jaccard et al., 2014). Paleorecords provide an important archive to investigate temporal and spatial scales of changes to marine oxygenation. In general, warm intervals during the late Quaternary were associated with decreased global ocean oxygenation and cool intervals were associated with increased oxygenation (Cannariato & Kennett, 1999; Cardich et al., 2019; Erdem et al., 2019; Jaccard et al., 2014; Praetorius et al., 2015). The Holocene is an ideal epoch to investigate changes in marine oxygenation because it has well documented intervals of oceanographic change and provides an opportunity to investigate ecological response to stress, including changes to temperature, oxygenation, carbon cycling and ocean circulation (Addison et al., 2017; Barron et al., 2003; Fisler & Hendy, 2008; Moffitt et al., 2015; Praetorius et al., 2015). Over millennial timescales, significant work along the California margin has documented paleoceanographic changes in coastal basins and within the bounds of the modern OMZ (Balestra et al., 2018; Cannariato & Kennett, 1999; Moffitt et al., 2014; Taylor et al., 2015). However, additional work is needed to constrain the timing and extent of oxygenation change below 1000 m, the relative impacts of surface processes and source waters on seafloor oxygenation, and how oxygenation at these depths responds to global and regional environmental change.

1.2 Southern California modern and paleoceanography

In the modern Northeast Pacific eastern boundary upwelling system, an OMZ exists at approximately 500 – 1000 m water depth and is an important driver of ecosystem zonation (Helly & Levin, 2004; Stramma, Johnson, et al., 2010). The combination of high productivity, high export of organic matter, and the age of

water masses entering the North Pacific at depth make this a particularly thick and laterally extensive OMZ (Bograd et al., 2008, 2019; Evans et al., 2020). The California Margin OMZ is expanding in intensity (decreases in dissolved oxygen), horizontal extent, and vertical thickness (shoaling) (Schmidtko et al., 2017; Stramma, Johnson, et al., 2010) caused by reductions in the oxygenation of source water and reduced ventilation due to surface warming and stratification (Bograd et al., 2008; Evans et al., 2020). Off the coast of California, dissolved oxygen decreased at a rate of up to 2.1 μmol/kg/year from 1984-2006 in the upper 500 m of the water column (Bograd et al., 2008, 2015). In the Southern California Current System, 81% of observed from 1993-2018 can be attributed to changes in oxygenation of source waters even within the upper 400 m of the water column (Evans et al., 2020).

In the modern system, Southern California Borderlands surface water flow is counterclockwise, with the western margin dominated by the southward flowing California Current and the eastern margin driven by the northward-flowing California Countercurrent and Davidson Current. At depth, the California Undercurrent flows south to north and is comprised of a mix of Southern Component Intermediate Water from the eastern tropical Pacific and northerly sourced North Pacific Intermediate Water (Balestra et al., 2018; Bograd et al., 2019; Checkley & Barth, 2009; Stott et al., 2000; Talley, 1993). Offshore Southern California, a series of submarine basins, generally deepening from north to south, structure intermediate and deep-water flow (Berelson, 1991; Berelson & Stott, 2003). Oxygenation in basinal environments is impacted by the export of organic matter from overlying surface waters, advection of intermediate and deep waters that spill into the basin, and within basin processes, including sediment and pelagic biogeochemical cycles. By examining the environments of multiple silled basins, the effects of water advection can be separated from surface processes and the depths of significant biogeochemical change can be determined.

The California margin OMZ fluctuated throughout the Holocene (Balestra et al., 2018; Christensen et al., 1994; McGann, 2011; Moffitt et al., 2014; Palmer et al., 2020). Previous analyses of marine sediment cores from the Santa Barbara Basin (SBB) document intervals of hypoxia in the early Holocene (11.5-10 ka) followed by oscillations in the strength of the OMZ from 10-6 ka with several intervals of hypoxia (less than 0.5 ml L^{-1} [O_2]) and an increase in oxygenation in the last 6 ka within SBB, yet the OMZ persists throughout the Holocene (Moffitt et al., 2014; Ohkushi et al., 2013; Wang et al., 2020). In Santa Monica Basin (SMB), severe hypoxia (less than 0.3 ml L^{-1} [O_2]) was present from the start of the Holocene to 9 ka, and the mid to late Holocene (9-0 ka) had weaker hypoxia (0.3-1.5 ml L^{-1} [O_2]) than the early Holocene (Balestra et al., 2018). The modern OMZ, with oxygen levels at 0-1.5 ml L^{-1} [O_2], developed in the mid to late Holocene (by 6-4 ka) across the broader North Pacific (Addison et al., 2017;

McGann, 2011; Ohkushi et al., 2013; Praetorius et al., 2015). Over the past several centuries the SMB experienced variable degrees of dysoxia at interannual to interdecadal time scales (Christensen et al., 1994). These changes are attributable to variable biological carbon flux and respiration at depth (Berelson and Stott, 2003; Stott et al, 2000), underscoring how sensitive the shallow-silled basins are to small changes in biological productivity. Previous analysis of ecosystem responses (benthic foraminiferal and invertebrate) to oxygenation change through the Holocene from the SBB indicate that intervals within the Holocene exhibit distinct phases of ecosystems that do not repeat or overlap, as the oxygen minimum zone and carbon maximum zone fluctuate (Moffitt et al., 2015; Myhre et al., 2017).

Here, we utilize records from three offshore basins to constrain changes in ocean oxygenation through the Holocene and resultant impacts on benthic ecosystems. Silled basins provide a unique opportunity to examine both local changes within each basin and to compare oxygenation history across depths when records overlap temporally. Combining a series of silled basins allows for the examination of change through time at multiple water depths and sill depths to investigate the relative impact of surface processes and intermediate water changes in determining oxygenation at depth (Balestra et al., 2018; Moffitt et al., 2014; Wang et al., 2020).

1.3 Benthic foraminiferal assemblages as a metric of past oxygenation and organic matter export

Benthic foraminiferal assemblages are an effective and established metric to quantify past changes in marine oxygenation (Balestra et al., 2018; Belanger et al., 2020; Bernhard & Gupta, 1999; Cardich et al., 2015, 2019; Caulle et al., 2014; De & Gupta, 2010; Kaiho, 1994; Moffitt et al., 2014; Murgese & De Deckker, 2005; Ohkushi et al., 2013; Praetorius et al., 2015). Benthic foraminiferal assemblages are sensitive to small changes in oxygenation in the North Pacific, even in suboxic environments, not only across large biological thresholds of anoxic or sulfidic conditions (Sharon et al., 2021). Multiple methodologies are used to interpret past environmental change from benthic foraminiferal assemblages, which we introduce and review below.

Quantifying absolute and relative abundance of benthic foraminiferal species is an established and foundational method; typically, studies quantify species downcore and interpret trends through time using observational or statistical approaches (e.g. Moffitt et al., 2014; McGann, 2011; Gardner et al., 1988). Studies of modern benthic foraminifera from multiple depositional environments and oxygenation regimes have identified oxygenation affinity of benthic foraminiferal species that can be used as indicator species of change through time; this method is most useful to reconstruct relative oxygenation or to

identify past oxygenation thresholds (e.g. Cannariato and Kennett, 1999; Palmer et al., 2020; Balestra et al., 2018; Bernhard and Gupta, 1999).

While these approaches provide relative oxygenation history, transfer functions are used to translate whole or partial benthic species assemblages into absolute oxygenation values (Behl & Kennett, 1996; Kaiho, 1994, 1999; McGann, 2011; Moffitt et al., 2014; Ohkushi et al., 2013; Sharon et al., 2021). Multi-species transfer functions including the Kaiho Benthic Foraminiferal Oxygenation Index, Behl Dissolved Oxygen Index, Schmidel Dissolved Oxygen Index, and Sharon-Behl Dissolved Oxygen Index are used to generate absolute values of past oxygenation by transforming the relative abundance of species into ml L^{-1} [O_2] (Kaiho, 1994; Ohkushi et al., 2013; Sharon et al., 2021). Transfer functions have typically been constructed using case studies from very low oxygen environments (such as Santa Barbara Basin) or by using the lowest known oxygen tolerance for a species (Kaiho, 1994; Ohkushi et al., 2013; Sharon et al., 2021). This approach generates inherently conservative predictions of oxygenation. Categorization of species into oxic, intermediate hypoxic, and anoxic environments used in both transfer functions and as indicator species varies by author (Cannariato & Kennett, 1999; Kaiho, 1994; Moffitt et al., 2014; Palmer et al., 2020; Praetorius et al., 2015). Here we follow the convention: weakly suboxic/oxic ([O2] >1.5 ml L^{-1}), intermediate hypoxic/suboxic ([O2] 1.5-0.5 ml L^{-1}), and sever hypoxic/dysoxic ([O2] <0.5 ml L^{-1}) (Moffitt et al., 2014; Palmer et al., 2020; Sharon et al., 2021; Tetard et al., 2021).

Recent work on paleoecological assemblages, including benthic foraminiferal assemblages, incorporating methodology from community ecology, including analysis of diversity, richness, and multidimensional statistical analysis, has expanded our breadth of understanding of how oxygenation impacts seafloor ecosystems (Belanger et al., 2020; Myhre et al., 2017; Sharon et al., 2021). Ecological analysis provides community-scale assessments of environmental change over time and often complements analysis of indicator taxa or transfer function calculations (Belanger et al., 2020; Myhre et al., 2017; Sharon et al., 2021). In addition to taxonomic evaluation of benthic foraminifera, studies are increasingly relying on morphometrics to assess past environments. These studies are predicated on biological morphological response or adaptation to oxygenation such as pore density, size, and shape (i.e., roundedness) and are used in both taxon-specific and taxon-independent analyses (Keating-Bitonti & Payne, 2016, 2018; Keating-Bitonti & Payne, 2017; Rathburn et al., 2018; Tetard et al., 2021). Typically, smaller, thin-walled, elongate species are indicative of low oxygen environments in which high-surface area to volume ratio is advantageous, to maximize oxygen absorption, while in well oxygenated environments, larger, thick-walled and porcelaneous taxa with rounded shapes are dominant (Tetard et al., 2021).

Food availability, driven by the timing (pulsed vs. constant) and amount of export of organic matter, and water depth play an important role in structuring seafloor ecosystems, including benthic foraminiferal assemblages (Belanger et al., 2012, 2020; Kaiho, 1999; Venturelli et al., 2018). Here we employ multiple assemblage analyses to investigate cores from three silled basins in the Southern California Borderlands. By combining approaches listed above, we quantify changes in oxygenation below 1000 m, deconstruct surface vs. advective processes as drivers of change, and investigate changes in source waters. This multi-site, multi-faceted approach allows us to reconstruct change over time in each basin and to assess regional scale oxygenation and ventilation history of the Southern California Borderlands through the Holocene.

2 Methods

2.1 Study site

Cores were collected from three silled basins within the Southern California Borderlands (Figure 1). Tanner Basin is located west of the Channel Islands and is the farthest offshore. The basin has a sill depth of 1160 m and a bottom depth of approximately 1500 m (Figure 1). San Nicolas Island is located south of San Nicolas Island and west of San Clemente Island. The basin has a sill depth of 1100 m and a bottom depth of approximately 1800 m (Figure 1). San Clemente Basin is located south of San Clemente Island and is the deepest site explored here. The basin has a sill depth of 1815 m and a bottom depth of approximately 1950 m (Figure 1). The water depth of each core was assessed at time of core collection and bottom depths of each basin were measured using GeoMapApp.

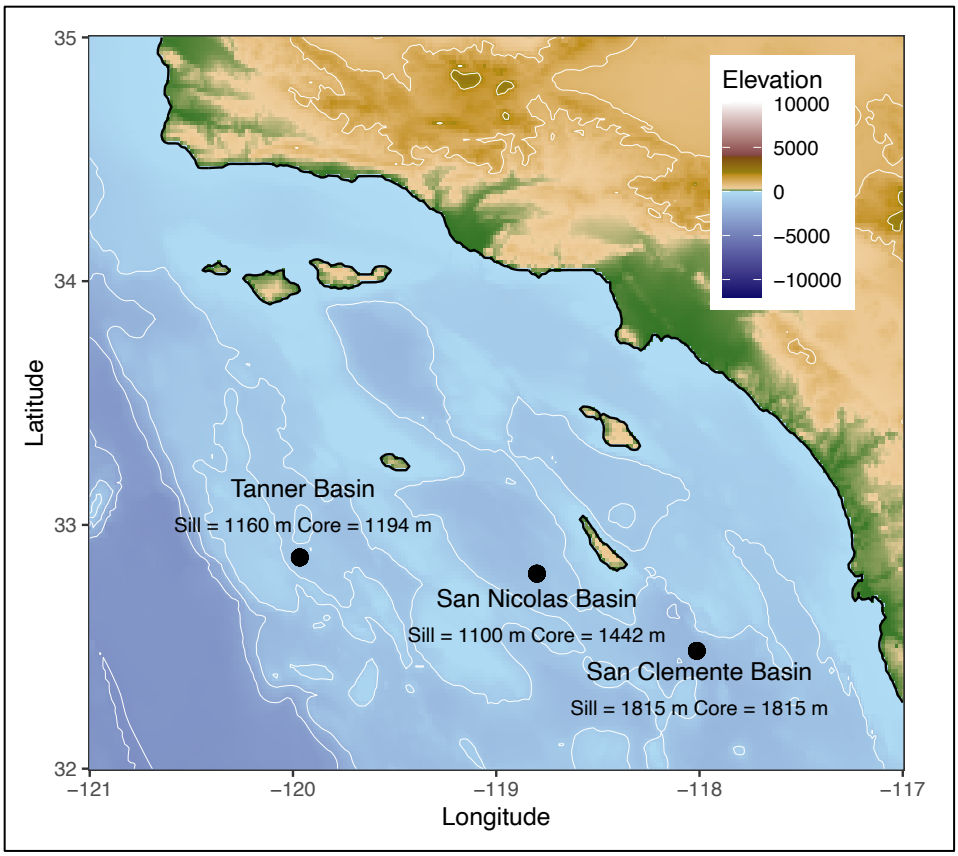

Figure 1: Map of the locations of the three cores used in this study. The sill depth and core collection depth for each core is reported in meters.

2.2 Sediment cores

We investigate three piston cores collected from the Southern California Borderlands on the Maurice Ewing Cruise 9504 in May - June 1995: EW 9504-09PC from Tanner Basin at 1194 m water depth, EW 9504-08PC from San Nicolas Basin at 1442 m water depth, and EW 9504-05 from San Clemente Basin at 1818 m water depth. All cores have 10.16 cm inner diameter. Cores were split on board the ship and were sampled at 2 cm intervals. All sample intervals used in this had an initial volume of 162.15 cm^3. Sediments from the working half of the core were disaggregated in sodium hexametaphosphate washed over a 63 µm sieve (see Stott et al. 2000). Sediments were dried and stored in glass vials at the University of Southern California until they were processed for this study. EW 9504-09PC (Tanner Basin) was examined from 0-40 cm at 2 cm intervals; intervals below 40 cm were not available for analysis. EW 9504-08PC (San Nicolas Basin) was examined at 2 cm intervals from 0-22 cm and every 6 cm from 24-64 cm. EW 9504-05 (San Clemente Basin) was examined at 2 cm intervals from 30-52 cm; intervals from 0-30 cm in EW9504-05 did not have sufficient foraminifera for robust analysis (see below) and were thus excluded from analysis.

233

234 **2.3 Radiocarbon dating and age model development**

235 Radiocarbon based age models were developed for each core using a combination of previously published
236 and newly generated planktic radiocarbon ages (Table S1, Figure S1). Five age dates within the Holocene
237 (1 San Clemente, 1 Tanner, 2 San Nicolas) were previously measured (Stott et al., 2000). These AMS ^{14}C
238 ages were completed using bulk planktonic foraminifera (weight ~3-5 mg) analyzed at the Lawrence
239 Livermore National Laboratory (Stott et al., 2000). Three additional radiocarbon dates (1 San Clemente, 2
240 Tanner, 1 San Nicolas) from bulk planktic foraminifera were analyzed in this study. All samples for
241 radiocarbon analysis were prepared by picking shell material from the >150 μm fraction, rinsing shells in
242 methanol, sonicating in methanol for 5-10 seconds, and rinsing twice with deionized water. Shells were
243 then dried in a 60^{O}C drying oven. Radiocarbon analysis was completed at the Lawrence Livermore
244 National Laboratory using $\delta^{13}C$ assumed values following the convention of Stuiver and Polach (1977).
245 The reported age is given in radiocarbon years using the Libby half-life of 5568 years. The Calib7.1
246 calibration program was used to calibrate ages using a reservoir age of 220.0 +/- 40.0 (Ingram & Southon,
247 1996; Stuiver & Polach, 1977). The age model for each core was generated using liner interpolation
248 between radiocarbon age dates (Table S1, Figure S1).

249

250 **2.4 Stable Isotope Analysis**

251 Stable isotope analyses from planktic and benthic foraminifera from EW9504-09 (Tanner Basin) were
252 conducted on *Globigerina bulloides* planktic foraminifera and *Cibicides mckannai* benthic foraminifera
253 from 0-40 cm at 2 cm intervals. Samples were prepared by picking from the >150 μm size fraction (2-5
254 individual *C. mckannai* per interval, 15-25 *G. bulloides* per interval), rinsing in methanol, sonicating in
255 methanol for 5-10 seconds, and rinsing twice with deionized water. Planktic foraminifera were analyzed
256 for $\delta^{18}O$ and $\delta^{13}C$ at the UC Davis Stable Isotope Laboratory and benthic foraminifera were analyzed at
257 the UC Santa Cruz Stable Isotope Laboratory.

258

259 Planktic carbon and oxygen isotope samples were analyzed using a GasBench II system interfaced with a
260 Delta V Plus Isotope Ratio Mass Spectrometer at the UC Davis Stable Isotope Laboratory using standard
261 UCD-SM92 (-1.94 for $\delta^{18}O$ and 2.08‰ $\delta^{13}C$) (Ostermann 2000). Values for $\delta^{13}C$ and $\delta^{18}O$ are expressed
262 in per mil (‰) relative to Vienna Pee Dee Belemnite, and values are corrected for changes in linearity and
263 instrumental drift. Benthic carbon and oxygen isotope samples were analyzed at the UC Santa Cruz Stable
264 Isotope Laboratory by acid digestion using an individual vial acid drop Themo Scientific Kiel IV
265 carbonate device interfaced to Thermo Scientific MAT 253 dual-inlet isotope ratio mass spectrometer. All
266 samples were measured with several replicates of the externally calibrated Carrera Marble in-house

standard reference material 'CM12' and the NBS-18 limestone international standard reference material. Values for $\delta^{13}C$ and $\delta^{18}O$ are expressed in per mil (‰) relative to Vienna Pee Dee Belemnite, and values are corrected for changes in linearity and instrumental drift. Data were combined with previously published records of planktic oxygen isotopes and benthic oxygen and carbon isotopes from the same core examined here (EW9504-09) to increase replicates in the late Holocene and to extend the record through the entire Holocene (Stott et al., 2000). As such, isotope records reflect analyses from three different laboratories.

2.5 Benthic Foraminiferal Assemblages

Samples were dry sieved over a 150 μm sieve and picked for benthic foraminiferal microfossils. Foraminifera greater than 150 μm have been documented to capture the range of environmental variability in paleoceanographic reconstructions as well as assemblages containing smaller foraminifera and the use of larger specimens results in reduced error in identification (Cannariato & Kennett, 1999; Caulle et al., 2014; Fenton et al., 2018; Palmer et al., 2020; Sharon et al., 2021). Individual foraminifera were picked and identified from each interval to obtain >100 individuals per sample (Kemp et al., 2020), yet two samples with 90 and 93 individuals available were included, as sample sizes as low as 58 have been shown to have stable assemblages (Belanger et al., 2020; Forcino et al., 2015). The average number of individual foraminifera identified in each interval was 230, with a range of 90-665. Samples were mounted on micropaleontology slides using gum tragacanth at time of identification and are archived in the Ocean Climate Laboratory at the UC Davis Bodega Marine Laboratory. Cores were not laminated; thus, bioturbation is expected and may have had an averaging effect on assemblages.

2.6 Foraminiferal morphometrics

Morphometrics of benthic foraminifera, including length, width, and surface area were measured using ImageJ software. Length and width of each individual was measured to the longest and widest margins of the shell. Three species were selected for analysis to represent a gradient of oxygenation affinity: *Quinqueloculina* sp. is weakly suboxic/oxic and *B. spissa* and *U. peregrina* are categorized as suboxic (Table S2). Measurements of *Quinqueloculina* sp. and *B. spissa* were quantified in Tanner Basin at 2 cm intervals from 0-40 cm, measurements of *Quinqueloculina* sp. and *U. peregrina* were quantified in San Clemente Basin at 2 cm intervals from 30-44 cm. From each interval, 5-25 individual shells were measured (based on availability of taxa). Results of morphometric analysis were compared to morphometric data (collected using the same methodology) from five open coastal margin sites (300-1175m) near San Diego (Palmer unpublished data), see Palmer et al., 2020 for further explanation of the open margin study site.

301

302 **2.7 Metazoan microfossil assemblages**

303 In addition to picking and identifying benthic foraminifera, ostracods (Arthropoda - Ostracoda) and
304 urchin spines (Echinodermata) were picked from the 150 μm sediment fraction at all intervals examined.
305 Samples were mounted on micropaleontology slides using gum tragacanth at time of identification and
306 are archived in the Ocean Climate Laboratory at the UC Davis Bodega Marine Laboratory. Due to low
307 abundances, presence/absence is recorded, rather than relative abundance.

308

309 **2.8 Benthic foraminiferal oxygenation index**

310 Oxygenation was reconstructed using two modified benthic foraminiferal oxygenation indices: Sharon-
311 Behl and Schmidel. Using a combination of paleo and modern samples, Sharon et al., 2021 modified the
312 Behl Dissolved Oxygen Index to allow for the inclusion of more species, thus allowing for its application
313 in a broader range of seafloor environments (Sharon et al., 2021). Here we further modified each by
314 adding ten additional species to the Sharon-Behl Dissolved Oxygen Index list of species using previously
315 published oxygenation affiliations and morphometric or taxonomic similarities (Table S2). Oxygenation
316 reconstructions were calculated using two equations: Sharon-Behl DO index = ((dysoxic % * 0.1) +
317 (suboxic % * 0.5) + (weakly suboxic/oxic % * 1.5))/100 and Schmidel index = ((weakly suboxic/oxic
318 %)/(weakly suboxic/oxic % + hypoxic %) + diversity (H`)) * 0.5 (Ohkushi et al., 2013).

319

320 **2.9 Statistical analysis**

321 Diversity of each interval of each core was calculated using Shannon Index (H). Richness was calculated
322 by tabulating the number of distinct species present in an interval. Non-metric multidimensional scaling
323 ordination, using square root transformation of assemblage species counts and Bray-Curtis similarities,
324 and cluster analysis were completed to identify relatedness between assemblages through time. All
325 multivariate analyses were completed using the Vegan R package (Myhre et al., 2017; Oksanen et al.,
326 2013). We used a single factor ANOVA to determine if there were significant differences among mean
327 morphometrics (length, width, surface area), diversity between basins, and values of reconstructed vs.
328 modern oxygenation. If the results of ANOVA were significant, we performed Tukey's Test to determine
329 where differences in the means occurred.

330

331 **2.10 Modern oxygenation data**

332 Modern oxygen data were sourced from the California Cooperative Oceanic Fisheries Investigations for
333 the years 1949-2019. Data were included from all sites in the CalCOFI sampling grid bounded by -116-

-121 W longitude and 32 – 34.5 N latitude (Point Conception is northern boundary)) and depths 1000-2000 m to maximize data availability. Oxygenation was calculated using Winkler Titration of bottle samples at the Scripps Institution of Oceanography (Bograd et al., 2003; Bograd & Lynn, 2003). Flagged data from CALCOFI and property-property and time series analysis excluded 19 data points. The CALCOFI data set used here includes a total of 272 modern oxygen measurements.

3 Results

3.1 Age Model Development

Radiocarbon ages (14C) were converted to calendar age using the Calib7.1 calibration program and a reservoir age of 220.0 +/- 40.0 (Ingram & Southon, 1996; Stuiver & Polach, 1977). Subsequently an age model for each core was generated using liner interpolation between dated intervals. Sedimentation rates were similar between basins and remained relatively constant through the Holocene: Tanner Basin sedimentation rate was 10.7 cm/kyr from 5.5 ka-1.9 ka, San Nicolas sedimentation rate was 10.3 cm/kyr from 11.9 ka- 5.4 ka and 8.9 cm/kyr from 5.4-2.9 ka, and San Clemente sedimentation rate was 5.3 cm/kyr from 12.7-1.4 ka (see Table S1 for radiocarbon ages and error and Figure S1). Sedimentation rate decreased with water depth, as expected. Coherence of age model within each core and between cores supports use of this age model (Figure S1). All following results are discussed as age in thousands of years before present (ka).

3.2 Stable isotope record

Stable isotope records from Tanner Basin varied slightly through time (Figure 3). Analysis of planktic oxygen and carbon isotopes from *G. bulloides* yielded the following: $\delta^{13}C$ mean is -0.59 (± 1σ = 0.25), range is -0.92 to -0.05, $\delta^{18}O$ mean is 0.22 (± 1σ = 0.31), range is -0.15 to 1.08 (Figure 3). Analysis of benthic oxygen and carbon isotopes from *C. mckannai* yielded the following: $\delta^{13}C$ mean is -0.03 (± 1σ =0.07), range is -0.13 to 0.10, $\delta^{18}O$ mean is 2.53 (± 1σ = 0.17), range is 2.29 to 2.73 (Figure 3).

3.3 Benthic foraminiferal assemblages

Benthic foraminiferal assemblages were quantified down core for each core in which sufficient benthic foraminifera were present (Tanner Basin 0-40 cm at 2 cm intervals, San Nicolas Basin 0-22 cm at 2 cm intervals, 24-66 at 6 cm intervals, San Clemente Basin 30-54 cm at 2 cm intervals). The total number of species (richness) in each sample ranged from 15 to 24 and species diversity (Shannon Index, H) ranged from 2.12 to 2.68, with a mean of 2.40 (± 1σ = 0.15) across all three basins. Species diversity (H) is significantly higher in Tanner Basin (mean=2.51, ± 0.11), relative to San Nicolas Basin (mean=2.30, ± 1σ = 0.11) and San Clemente Basin (mean=2.37, ± 1σ = 0.10) (ANOVA, Tukey Test $p<0.05$) (Figure S4).

Comparison of diversity through time in individual basins using 0.5 or 1 ka time bins shows that diversity (H) is not statistically different through time in Tanner ($p>0.05$), San Nicolas ($p>0.05$), and San Clemente ($p>0.05$) basins. Multivariate statistical analysis using nonmetric multidimensional scaling (NMDS) of down-core assemblages shows that, through time, assemblage similarity within sites exceeds similarity to assemblages at any other site (Figure S2).

In Tanner Basin, the most common species (in descending order) are *B. spissa, G. subglobosa, H. soldanii, Quinqueloculina* sp., and *P. murrhina* (Figure 2). Species diversity (H) ranged from 2.12-2.68 with a mean of 2.51 ($\pm 1\sigma = 0.11$) (Figure S4); diversity did not change significantly through time when considered at 0.5 or 1 ka time intervals (ANOVA, $p>0.05$). The benthic foraminiferal assemblage gradually changed from 5.5 – 1.9 ka. Cluster analysis with 50% similarity identifies two cohorts of benthic assemblages in Tanner Basin separated in time from 5.5 – 4.0 ka and 4.0 – 1.9 ka (Figure S2). Comparison of NMDS with cluster analysis and individual species plot shows this shift is largely driven by a gradual increase in *Hansenisca soldanii* (previously *Gyroidina soldanii*) and decrease in *B. spissa* and *U. peregrina* from 5.5 to 1.9 ka (Figure 2, S2). *G. subglobosa* and *Quinqueloculina* sp consistently make up 10-20% of the assemblage through time (Figure 2).

In San Nicolas Basin, the most common species (in descending order) are *U. peregrina, E. pacifica, C. mckannai, B. spissa,* and *Uvigerina* sp (Figure 2). Species diversity (H) ranges from 2.12-2.56 with a mean of 2.30 ($\pm$ 0.11) (Figure S4); diversity did not change significantly through time when considered at 0.5 or 1 ka time intervals (ANOVA, $p>0.05$). The assemblage in San Nicolas Basin exhibits little change through time from 10.1-4.7 ka when *U. peregrina* makes up 15-45% of the assemblage. From 4.7-4.2 ka, there is a sharp decline in *U. peregrina* and a sharp increase in *C. mckannai* (Figure 2). From 4.0-1.9 ka, the trend reverses, and the assemblage is very similar to the assemblage from 10.1-4.7 ka. NMDS and cluster analysis (with 50% similarity) identify an anomalous period in San Nicolas Basin from 4.7-4.2 ka that is different from the time points before and after this period (Figure 2, S2).

In San Clemente Basin, the most common species (in descending order) are *U. peregrina, C. mckannai, E. pacifica, Quinqueloculina* sp., and *Uvigerina* sp (Figure 2). Species diversity (H) ranges from 2.17-2.51 with a mean of 2.37 ($\pm$ 0.10) (Figure S4); diversity did not change significantly through time when considered at 0.5 or 1 ka time intervals (ANOVA, $p>0.05$). In San Clemente Basin, relative abundance of benthic foraminifera exhibits little change over time from 11.2-7.1 ka as shown by both individual species analysis and NMDS. Cluster analysis shows the assemblage is 50% similar through all time intervals examined (Figure 2, S2).

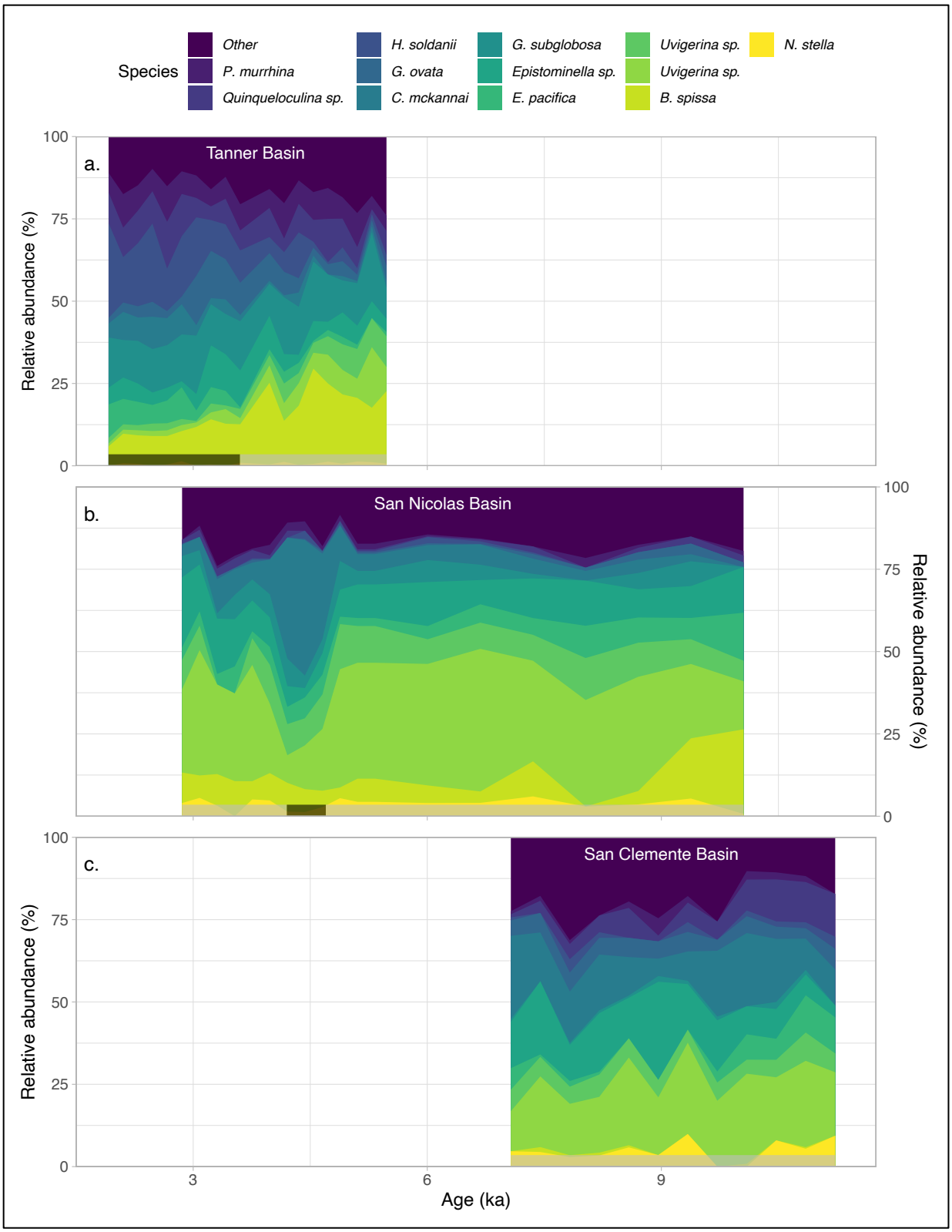

Figure 2: Relative abundance of benthic foraminifera vs. age in thousands of years before present for three cores examined here: Tanner (a.), San Nicolas (b.), and San Clemente (c.). Ten most abundant

species are shown; all other species grouped as "other." Each color represents a taxonomic group (species, genus, or other). See legend at top of plot for color of each. Taxa colors are ordered from dysoxic indicator taxa (yellow/bottom of plot) to oxic indicator taxa (blue/top of plot). Color bars across bottom of each plot represent cohorts with 50% similarity following NMDS and cluster analysis for each individual basin (Figure S2).

3.4 Metazoan microfossil analysis

Urchin spines and ostracods were present in the Tanner Basin core, but do not present a coeval trend; urchins are present in 13 of 19 intervals, ostracods are present in 5 of 19 samples. Urchin spines and ostracods were scarce in sediments from San Nicolas Basin: urchin spines are present in 6 of 17 and ostracods are present in 2 of 17 intervals. Ostracods and urchin spines were nearly ubiquitous (present in every interval except one) in San Clemente Basin (Figure S5).

3.5 Shell morphometrics

Shell size, measured as length, width, and surface area of three taxa (*U. peregrina, Quinqueloculina* sp., and *B. spissa*) was compared across the three cores examined here and to unpublished size data from a suite of cores from the San Diego Margin (Palmer et al., 2020). Shell size of *U. peregrina* is statistically significantly larger in coastal sites ($p<0.05$) relative to San Clemente basin (Figure S3a). Shell size of *B. spissa* is statistically significantly larger in coastal sites ($p<0.05$) relative to Tanner basin (Figure S3a). Shell size of *B. spissa* and *Quinqueloculina* from Tanner Basin show relatively little variability through time (5.5-1.9 ka) (Figure S3b, c). As all metrics of shell size (length, width, and surface area) show the same trends, further discussion uses only shell surface area as a metric of whole shell size.

3.6 Reconstructed oxygenation using transfer functions

Reconstructed dissolved oxygen using the modified Sharon-Behl Index ranges from 0.56-1.12 ml L^{-1} with a mean of 0.79 ml L^{-1} (Figure S4) and varies across basins: Tanner Basin mean is 0.86 ml L^{-1} and ranges from 0.59-1.20 ml L^{-1}, San Nicolas Basin mean is 0.67 ml L^{-1} and ranges from 0.56-1.02 ml L^{-1}, and San Clemente Basin mean is 0.84 ml L^{-1} and ranges from 0.68-0.96 ml L^{-1}. Reconstructed dissolved oxygen using the Schmidel Index ranges from 1.36-1.81 ml L^{-1} for all three cores, with a mean of 1.62 ml L^{-1} (Figure S4). Schmidel Index reconstructed oxygenation varies across basins: Tanner Basin mean is 1.73 ml L^{-1} and ranges from 1.59-1.81 ml L^{-1}, San Nicolas Basin mean is 1.50 ml L^{-1} and ranges from 1.36-1.66 ml L^{-1}, and San Clemente Basin mean is 1.60 ml L^{-1} and ranges from 1.48-1.71 ml L^{-1}.

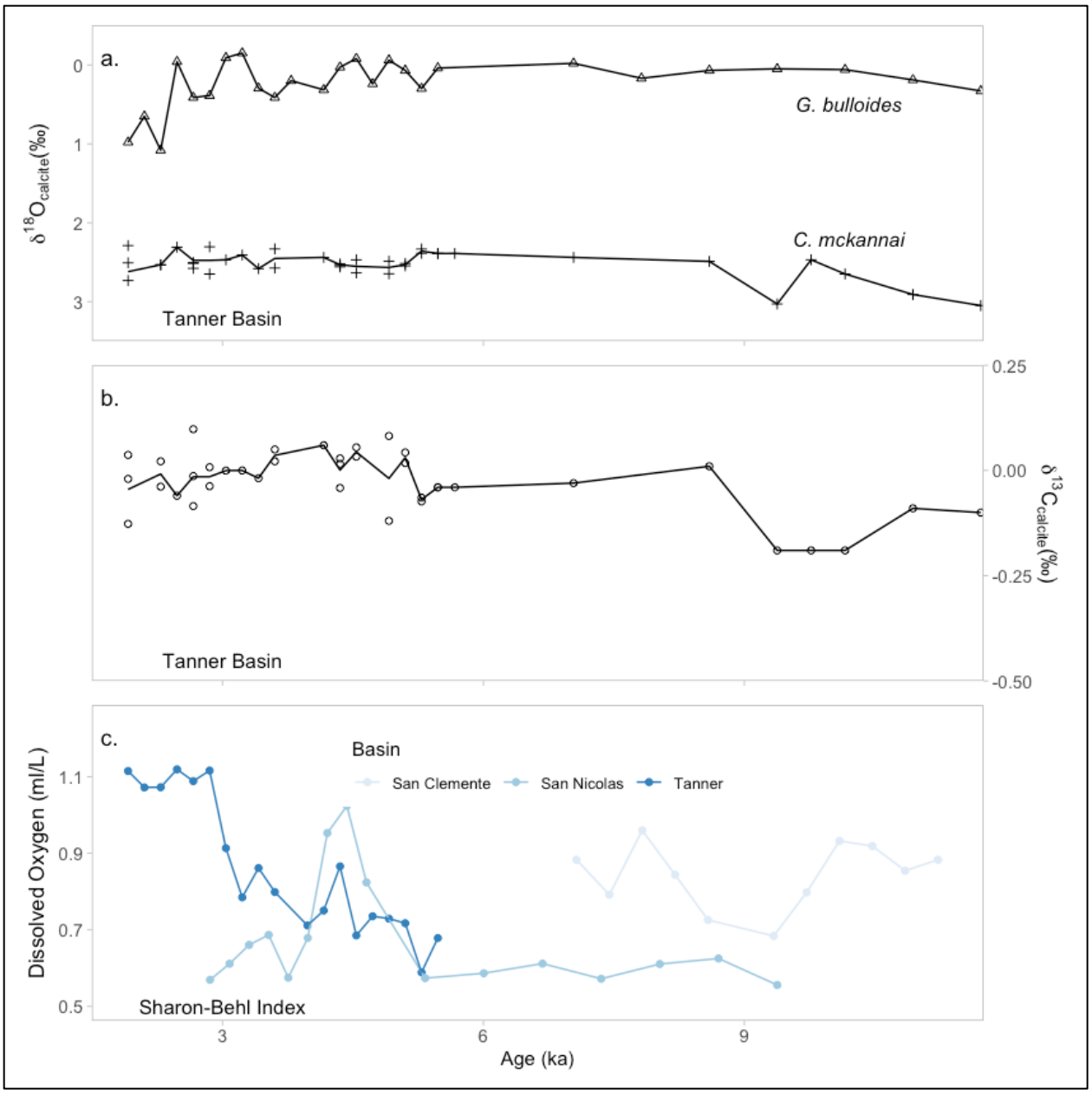

Figure 3: Stable isotope record from Tanner Basin and reconstructed oxygenation for all three sites using modified Sharon-Behl Dissolved Oxygen Index. Oxygen isotopes of planktic foraminifera *G. bulloides* from this study and Stott et al., 2000 indicated as triangles (a.). Oxygen and carbon isotopes of benthic foraminifera *C. mckannai* from this study and Stott et al., 2000 indicated as + (b.). In both isotope figures, data from 5.5-1.9 ka includes both data from Stott et al., 2000 and this study, data from 11.7-5.5 from Stott et al., 2000. Reconstructed dissolved oxygen content in each basin (Tanner, San Nicolas, San Clemente) using modified Sharon-Behl Dissolved Oxygen Index (c.). Oxygen in ml L^{-1}.

3.7 Modern oxygenation in the Southern California Borderlands and comparison to reconstructed oxygenation

Modern oxygenation decreases linearly with depth from 1000 to 2000 m in this region, and ranges from 0.15-1.67 ml L^{-1} and a mean of 0.78 ml L^{-1} across all depths (1000-2000m). Modern oxygenation in the 50 m above and below the Tanner Basin site (1144-1244 m) has a mean of 0.77 ± 0.18 ml L^{-1}. Modern oxygenation in the 50 m above and below the San Nicolas Basin site (1392-1492 m) has a mean of 0.88 ± 0.37 ml L^{-1}. Modern oxygenation in the 50 m above and below the San Nicolas Basin site (1392-1492 m) has a mean of 1.51 ± 0.09 ml L^{-1}.

4 Discussion

4.1 Benthic foraminiferal assemblages as paleo-oxygenation proxy

By analyzing the complete assemblage from each basin, we interpret a gradual shift in relative abundance of taxa in Tanner Basin, multi-centennial shifts in the assemblage at San Nicolas Basin, and stability in the assemblage in San Clemente Basin. Examining indicator taxa, we identify a decrease in hypoxic taxon *B. spissa* and a decrease in *U. peregrina* coeval with an increase in oxic indicator *Hansenisca* sp. in Tanner Basin from 5.5 to 1.9 ka. In San Nicolas Basin, we observe a short period of divergence from the mean assemblage driven by an increase in the oxic-associated taxon *C. mckannai* and a sharp decline in *U. peregrina* from 4.7-4.2 ka. We observe little change over time in the relative abundance of these indicator taxa in San Clemente Basin.

Reconstructed oxygen concentration differs between the two transfer functions compared here. Reconstructed dissolved oxygen using Sharon-Behl Index for all three cores yields values (0.56-1.12 ml L^{-1}) within "intermediate hypoxia" as defined by Moffitt et al., 2014 and "suboxic" as defined by Cannariato and Kennett 1999 and Kaiho 1994. Reconstructed values using the Sharon-Behl Index are similar to the range of modern values for bottom water oxygenation with notable exceptions discussed below (Figure 4b, c). In comparison, the Schmidel Index output is higher (1.36-1.81 ml L^{-1}) than the Sharon-Behl Index by approximately 0.5 ml L^{-1}, and it does not capture the variability seen in the full assemblage (Figure S4). We posit that this is due to the fact that diversity and oxygenation are not necessarily inversely correlated, particularly in intermediate hypoxic environments, yet the Schmidel Index is based on diversity. Across taxa and faunal size, diversity is typically low within oxygen minimum zones (Levin, 2003). For benthic foraminifera in dysoxic basins specifically, typically density is high, and diversity is low (Levin, 2003; Moffitt et al., 2014). Yet, other parameters such as proximity to the margin of the OMZ, sediment grain size, and organic matter availability also play important roles in structuring foraminiferal diversity. Further, oxygenation plays a more dominant role in structuring

diversity across biological thresholds (such as below 0.5 ml L-1 [O_2]) than across oxygen gradients that do not cross biological thresholds (McGann, 2011; Palmer et al., 2020; Sharon et al., 2021; Venturelli et al., 2018). Thus, we utilize the modified Sharon-Behl Index to reconstruct absolute values of paleo-oxygenation (Figure 3).

Community-level changes are tracked by diversity and multi-dimensional community metrics. Diversity varied little between basins and through time within each basin. Shannon Index of diversity (H) ranged from 2.12 to 2.68 across all sites and points in time, and diversity did not significantly change through time at any site across this interval (ANOVA, $p>0.05$) (Figure S4). We hypothesize that the stability in diversity indicates that environmental conditions were also relatively stable through this interval. This evidence aligns with results of oxygenation reconstruction in the suboxic/intermediate hypoxic category from the Sharon-Behl Index throughout all records examined here (Figure 3). Results of multi-dimensional analysis show species assemblages are distinct in each basin; NMDS and 50% similarity analysis demonstrates that at any time point, assemblages are more similar to other time points from the same basin than to any other time point from an adjacent basin (Figure S2). This demonstrates that each basinal environment is unique and the analysis of benthic foraminifera as environmental indicators must consider local factors.

Changes in benthic foraminifera morphology can reflect environmental variations that are missed by community-based analyses. Comparison of two species (*U. peregrina*, *B. spissa*) between basins (studied here) and open margin sediments (San Diego Margin, see Palmer et al., 2020) shows that both species are larger in the nearshore environment relative to offshore basins (Figure S3). At this scale, we interpret the size difference to be representative of higher relative organic matter input at coastal margin sites in comparison to offshore basins. In comparison to changes across sites, there is relatively little change in shell size of *Quinqueloculina* sp. (oxic indicator species) or *B. spissa* (suboxic indicator species) over time (5.5-1.9 ka) in Tanner Basin (Figure S3).

4.2 Oxygenation and ventilation change in individual basins through the Holocene

4.2.1 Assemblage and environmental change through time in Tanner Basin

Planktic $\delta^{18}O$ records from Tanner Basin indicate constant sea surface conditions (salinity/temperature) through most of the Holocene (11.75 – 2.3 ka) and a decrease in sea surface temperature or increase in salinity from 2.3 – 1.9 ka relative to the rest of the Holocene (Figure 3). Benthic $\delta^{18}O$ and $\delta^{13}C$ of the epibenthic foraminifera *C. makannai* exhibit little change through the Holocene (Figure 4). In contrast, the benthic foraminiferal assemblage gradually shifts from more hypoxic to more oxic associated taxa

514 from 5.5ka to 1.9 ka (Figures 2, 3). Cluster analysis indicates two distinct cohorts (each with 50%
515 similarity in species) at 5.5-3.6 ka and 3.6-1.9 ka. This shift is largely driven by the increase in
516 *Hansenisca soldanii* (previously *Gyroidina soldanii*) and decrease in *B. spissa* and *U. peregrina* (Figure
517 2). *Hansenisca soldanii* has been documented in well oxygenated, oligotrophic, cold deep water with
518 pulsed food supply (De & Gupta, 2010), and both *B. spissa* and *U. peregrina* are well documented
519 indicators of low oxygen. Using the modified Sharon-Behl Index, reconstructed oxygenation increases
520 from 0.58 to 1.12 ml L^{-1} across this interval (Figure 3). Thus, we interpret this assemblage shift as an
521 indication of a gradual increase of approximately 0.4ml/L in Tanner Basin from 5.5 to 1.9 ka.
522
523 Downcore morphometric analysis shows that neither relative abundance nor surface area of
524 *Quinqueloculina* sp. (an oxic indicator species) changes through time. Although *B. spissa* decreases in
525 relative abundance from 5.5-1.9 ka, shell size (surface area) does not change through time (Figure S3).
526 Stability in shell size concurrent with changes in relative abundance may indicate an interaction of factors
527 including oxygen and organic matter influx in determining lethal vs. sublethal effects on *B. spissa*.
528 Further, the lack of changes in shell size of *B. spissa* and *Quinqueloculina* across this interval may
529 indicate a consistent supply of surface -exported organic matter, the main food resource for these benthic
530 foraminifera. Ostracod and echinoderm presence are not correlated with increase in dissolved oxygen at
531 this site (Figure S5). We hypothesize that the shift identified in the benthic foraminiferal assemblage is in
532 response to a relatively small change in oxygenation (less than 1 ml L^{-1}) and does not represent
533 fluctuations across biologically important thresholds for metazoan taxa (oxygenation was never below 0.4
534 ml L^{-1}, Figure 3).
535
536 When compared to modern CalCOFI data, reconstructed oxygenation (using the Sharon-Behl Index) is
537 within 1σ of modern mean oxygenation (Figure 4), except for the interval from 3 – 1.9 ka in which
538 reconstructed oxygen is higher than modern by 0.3 ml L^{-1} (Figure 4). There is no significant difference
539 (ANOVA, Tukey, p=0.51) between reconstructed oxygenation values (mean=0.86 ml L^{-1}) and all modern
540 oxygenation values (mean=0.77 ml $L^{-}1$) within waters 50m above and below the Tanner Basin Site
541 (Figure 4). Combining assemblage, oxygenation index, and isotopic history of Tanner Basin, we identify
542 a gradual increase in oxygenation in the basin from 5.5-1.9 ka that is not correlated with changes in either
543 the oxygen or carbon isotope records and remains within the modern range of dissolved oxygen
544 variability. This increase in oxygenation is coeval with a decrease in the strength of the OMZ in the last 6
545 ka in Santa Barbara Basin, which has been shown to be driven by an increase in the oxygenation of North
546 Pacific Intermediate Water formation and ventilation relative to the early Holocene (Wang et al., 2020).
547 We hypothesize that the increase in oxygenation in Tanner Basin during the late Holocene is driven by an

increase in oxygenation of North Pacific Intermediate Water. Further, our data show that the changes in Tanner Basin dissolved oxygen are minor when compared to changes in oxygenation in nearby shallow basins still within the OMZ (Balestra et al., 2018; Moffitt et al., 2014; Palmer et al., 2020; Wang et al., 2020).

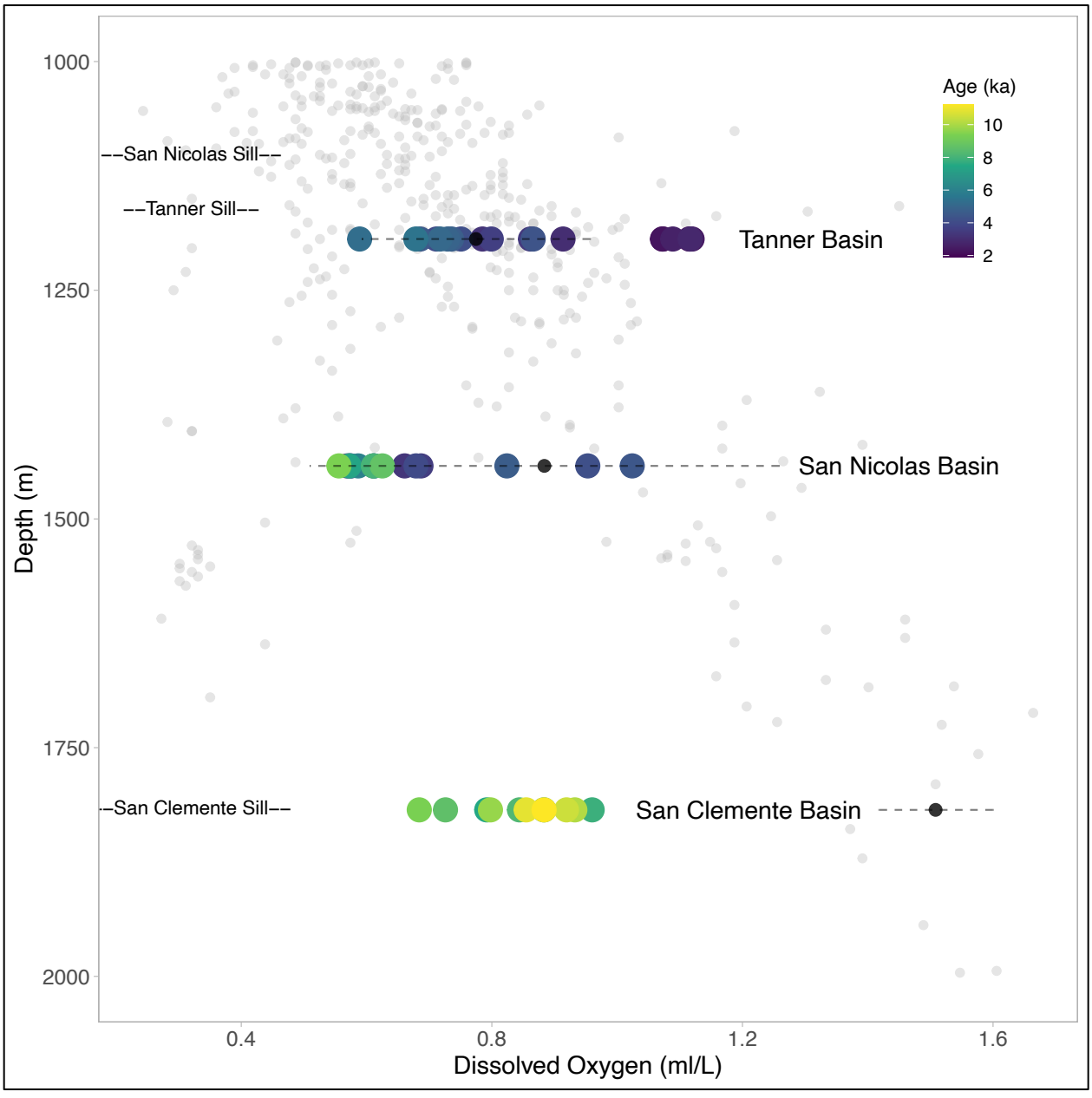

Figure 4: Reconstructed dissolved oxygen concentration (ml L^{-1}) from Tanner, San Nicolas, and San Clemente Basin (black dots) compared with modern dissolved oxygen concentration (ml L^{-1}) from CALCOFI bottle sampling (1986-2019) (gray dots). Depth of sill of each basin is labeled. Black dots show mean modern dissolved oxygen concentration from 50 m above and below each site and dashed gray line shows 1σ range in dissolved oxygen concentration from 50 m above and below each site.

558

559 **4.2.1 Assemblage and environmental change through time in San Nicolas Basin**

560 In San Nicolas Basin, low oxygen associated benthic foraminiferal taxa dominate from 10.0 to 4.7 ka. A
561 short period of anomalous assemblage driven by an increase in *C. mckannai,* an oxic-associated taxon,
562 and a sharp decline in *U. peregrina*, an intermediate hypoxia-associated taxon, occurs at 4.7-4.2 ka and is
563 interpreted as an interval of increased oxygenation. This interval is clear in both species-specific records
564 as well as through cluster analysis of the complete assemblage. Using the modified Sharon-Behl Index,
565 reconstructed oxygenation increases from 0.59 ml L^{-1} before the interval to a maximum of 1.03 ml L^{-1}
566 during the oxygenation interval (Figure 3). Oxygenation returned to pre-event levels of dissolved oxygen
567 after 4.2 ka and pre and post event assemblages are similar, indicating an absence of a legacy effect of the
568 event on the community (Figure 2). Metazoan invertebrate microfossils (ostracods and urchin spines) are
569 scarce in this core and changes in presence/absence of metazoans do not correlate with shifts in benthic
570 foraminiferal assemblages (Figure S5). Modern studies of circulation in San Nicolas Basin indicate that
571 residence time for bottom waters in the basin are 9 ± 2 months (Berelson, 1991). As such, we hypothesize
572 that the assemblage response recorded here represents persistent oxygenation or repeated ventilation on a
573 decadal-to centennial scale, rather than a single episode of ventilation. Yet, the absolute change in
574 oxygenation is relatively minor and still within a threshold of intermediate hypoxia and within the range
575 of modern values (Figure 3, 4).

576

577 When compared to modern CalCOFI data, reconstructed oxygenation in San Nicolas Basin is slightly
578 lower than modern mean dissolved oxygen yet remains within 1σ of the modern mean at all points
579 throughout the Holocene (Figure 4). Reconstructed oxygenation (mean=0.67 ml L^{-1}) is statistically lower
580 than modern oxygenation from waters 50m above and below the depth of the San Nicolas site (ANOVA,
581 Tukey $p<0.05$) (Figure 4). Further, reconstructed oxygenation in periods outside the event were similar to
582 modern oxygenation at the sill depth of San Nicolas Basin (1100m, see Figure 4). The scale of change in
583 reconstructed dissolved oxygen, relative abundance of species, and species diversity in San Nicolas Basin
584 across this interval of change is minor when compared to intervals of change in nearby basins across the
585 deglacial and in comparison to Holocene changes within basins that experienced shifts between anoxic
586 and oxic conditions, such as the Macoma Event in the Santa Barbara Basin (Balestra et al., 2018;
587 Cannariato & Kennett, 1999; Moffitt et al., 2015; Praetorius et al., 2015; Schimmelmann et al., 2013).

588

589 **4.2.1 Assemblage and environmental change through time in San Clemente Basin**

590 Environmental conditions remained relatively constant in San Clemente Basin from 11.2-7.1 ka as
591 demonstrated by the lack of variability in the benthic foraminiferal assemblages. Species diversity does

not change significantly through time (Figure S5). Reconstructed oxygenation from the modified Sharon-Behl Index ranges from 0.67 to 0.96 ml L^{-1} across this interval; this variability is reduced relative to Tanner and San Nicolas Basins (Figure 3). The assemblage at this depth is distinct from coastal margin environments and other, shallower basins (Balestra et al., 2018; Moffitt et al., 2014; Palmer et al., 2020). Ostracods and urchin spines are present in every interval (except one) examined here, indicating a well-oxygenated seafloor environment that supported metazoan life and motile organisms (Figure S5) (Moffitt et al., 2015). Ecological differences between the shallow sill basins (San Nicolas and Tanner) vs. the deep sill basin (San Clemente) documented here are mirrored in previously documented seafloor metazoan assemblages (France, 1994). We hypothesize that at 1815 m water depth, this site was not impacted by changes in the oxygen minimum zone during the Holocene and that intermediate and deep water reaching this site had a consistent source from 11.2-7.1 ka.

In comparison to modern CalCOFI data, reconstructed dissolved oxygen (mean=0.84 ml L^{-1}) in the early and mid-Holocene is statistically lower than modern dissolved oxygen (mean=1.50 ml L^{-1}) within 50m above and below the depth of the San Clemente Site ($p<0.05$) (Figure 4). We propose three potentially overlapping hypotheses for this difference. First, this may be an artifact of the Sharon-Behl Index, which uses lowest known thresholds of oxygenation and thus may predict the minima of dissolved oxygen concentrations. Second, in the early Holocene, sea level was lower than modern (by approximately 70 m) thus, the sites sampled here may have been less well oxygenated simply due to being at a shallower depth, but this would not explain the entire difference from modern (Figure 4) (Fleming et al., 1998; Moffitt et al., 2014). Finally, the preformed oxygenation of the incoming water masses may have been lower than modern, a pattern that is reflected in Santa Monica and Santa Barbara Basins at this time (Balestra et al., 2018; Wang et al., 2020).

4.3 Intermediate water change and basinal processes in Southern California Borderlands

In the early to mid-Holocene (11.2-4.7 ka), seafloor oxygenation below 1400 m was stable in the Southern CA Borderlands, evidenced by stability in assemblage records from San Clemente Basin (1815 m) and San Nicolas Basin (1442 m), and was likely driven by consistent source and composition of intermediate waters. Benthic foraminiferal assemblage records from the Santa Lucia Slope (ODP 1017, 955 m) offshore Point Conception indicate a stable suboxic environment through the early and mid-Holocene and are similar in taxonomic composition to our records from San Nicolas and San Clemente Basins (Cannariato & Kennett, 1999). Synchrony in stability and assemblages across San Nicolas Basin (1442 m), San Clemente Basin (1818 m), and the Santa Lucia Slope (955 m) contrasts with evidence of fluctuations in age of North Pacific Intermediate Water entering SBB (as recorded by benthic-planktic

radiocarbon age differences) at 9 ka (Roark et al., 2003), expansion of the OMZ in SBB in the early Holocene (Wang et al., 2020), and a turning point from hypoxic to suboxic conditions at 9 ka in Santa Monica Basin (indicated by benthic foraminiferal assemblages and geochemical records) (Balestra et al., 2018). Differences between sites can be explained by differences across water depth. We propose that changes in the source and strength of NPIW impacted sites at 400-1000m water depth (SBB, SMB) (Balestra et al., 2018; Roark et al., 2003; Wang et al., 2020), but had less of an effect on the water column below 1000 m.

In the mid to late Holocene, San Nicolas Basin experienced a multi-centennial oxygenation interval from 4.7-4.2 ka and oxygenation increased in Tanner Basin gradually from 5.0-1.9 ka. The interval of increased oxygen in San Nicolas Basin and the increasing oxygenation in Tanner Basin from 5.0-4.0 ka may be due to the same driver because their sill depths of each are similar, 1100 m and 1160 m respectively. Ventilation and oxygenation of these offshore basins is coeval with an increase in oxygenation in Santa Barbara Basin beginning around 6 ka that is attributed to the increasing strength and oxygenation of North Pacific Intermediate Water (Wang et al., 2020). Wang et al., 2020 identify sea ice formation and brine rejection in the North Pacific as the driver of increased oxygenation after 6 ka. We posit that the slight increase in oxygenation in both San Nicolas and Tanner basins may be due to increased oxygenation of North Pacific Intermediate Water entering both basins. After 4.0 ka, the trends diverge, and San Nicolas Basin returns to lower oxygenation levels. The difference in the two basins can be explained by basinal processes occurring at depth, a change in source or strength of influx of intermediate waters to San Nicolas Basin, or differences in surface water productivity due distinct overlying surface current processes. We present two hypotheses: first, both basins may have experienced “indirect” ventilation through diffusion of dissolved oxygen from overlying waters, rather than “direct” ventilation due to advection, thus explaining why increased oxygen is persistent in Tanner Basin but not San Nicolas Basin (Talley, 1993), or basinal processes due to the different shapes and depths of each basin may have impacted the oxygenation of each.

Although oxygenation does vary across the Holocene in Tanner, San Nicolas, and San Clemente basins, all variability was within 1 ml L^{-1} O_2 and does not cross critical biological thresholds below 0.5 ml L^{-1} or above 1.5 ml L^{-1} in any basin. As such, variability in oxygenation and ventilation of San Nicolas, Tanner, and San Clemente basins is reduced relative to shallower sites, including Santa Barbara Basin and Santa Monica Basin, across the entire Holocene (Balestra et al., 2018; Moffitt et al., 2014; Ohkushi et al., 2013). Additionally, Holocene-scale oxygenation changes (presented here) are reduced relative to glacial/interglacial changes in oxygenation in the basins examined here and in the nearby Santa Lucia

Slope (Cannariato & Kennett, 1999; Stott et al., 2000). This indicates that Holocene-scale climate changes driving oxygenation change shallower than 1000 m are not impacting waters below 1000 m and that climate changes within the Holocene do not significantly impact oxygenation below 1000 m, despite changes in the intensity and extent of the OMZ shallower than 1000 m. As such, we hypothesize that deoxygenation due to anthropogenic climate change will also have a greater impact on the water column above 1000 m and that source water oxygenation is a dominant driver of oxygenation at depth and must be considered when predicting future oxygenation change.

5 Conclusion

Reconstruction of past oxygenation using analysis of benthic microfaunal communities (foraminiferal and metazoan) is optimized by combining multiple approaches including analysis of indicator taxa, reconstruction of oxygenation using multi-taxa indices, and community scale-analysis such as multidimensional analysis and diversity. Here we demonstrate the utility of combined approaches, and we expand the use of the Sharon-Behl Index for paleo-oxygenation reconstruction. Analysis of benthic foraminiferal assemblages from three silled basins (Tanner, San Nicolas, San Clemente) in the Southern California Borderlands combined with benthic and planktic stable isotope analysis from Tanner Basin show a gradual increase (0.5 ml L^{-1} [O_2]) in oxygenation in Tanner Basin from 5.5-1.9 ka, multi-centennial variability in oxygenation (on the scale of 0.5 ml L^{-1} [O_2]) in San Nicolas Basin, and stability in the seafloor environment in San Clemente Basin from 11.2-7.1 ka, yet lower oxygenation relative to modern at this site. Holocene scale climate changes did not drive significant changes (> 1 ml L^{-1}) in marine oxygenation below 1000 m in the Southern California Borderlands. In the context of modern oxygenation changes, findings from this analysis show that Holocene-scale changes in seafloor oxygenation of the Southern California Borderlands below 1000 m has remined relatively stable and the variance across millennia is similar to decadal-scale variance in the modern ocean. As such, we expect that future changes to marine oxygenation will be greater at depths above 1000 m relative to deeper waters and note that if anthropogenic climate change induced changes in oxygenation do cause shifts in dissolved oxygen greater than > 1 ml L^{-1} below 1000 m, it will represent a divergence from scales of variability over the last 11 ka.

Acknowledgements

The authors declare no conflicts of interest. We acknowledge funding for this project provided through National Science Foundation Grant OCE 1832812 to TMH and PDR and the University of California, Davis Dissertation Year Grant and the University of California, Davis Earth and Planetary Sciences Durrell Fund Research Award. We thank Sarah Merolla and Kimberly Bowman for their support with sample preparation and processing.

Open Research

The benthic foraminiferal assemblage data, radiocarbon age model data, carbon and oxygen stable isotope data, and morphometric data used for environmental reconstruction in the study are available at Dryad via https://doi.org/10.6071/M3Q090 titled Data from: Oxygenation of offshore Southern California Marine Basins through the Holocene with CC0 1.0 license (Palmer et al., 2021).

References

Addison, J. A., Barron, J., Finney, B., Kusler, J., Bukry, D., Heusser, L. E., & Alexander, C. R. (2017). A Holocene record of ocean productivity and upwelling from the northern California continental slope. *Quaternary International*.

Balestra, B., Krupinski, N. B. Q., Erohina, T., Fessenden-Rahn, J., Rahn, T., & Paytan, A. (2018). Bottom-water oxygenation and environmental change in Santa Monica Basin, Southern California during the last 23 kyr. *Palaeogeography, Palaeoclimatology, Palaeoecology*, *490*, 17–37.

Barron, J. A., Heusser, L., Herbert, T., & Lyle, M. (2003). High-resolution climatic evolution of coastal northern California during the past 16,000 years. *Paleoceanography*, *18*(1).

Behl, R. J., & Kennett, J. P. (1996). Brief interstadial events in the Santa Barbara basin, NE Pacific, during the past 60 kyr. *Nature*, *379*(6562), 243–246. https://doi.org/DOI 10.1038/379243a0

Belanger, C. L., Jablonski, D., Roy, K., Berke, S. K., Krug, A. Z., & Valentine, J. W. (2012). Global environmental predictors of benthic marine biogeographic structure. *Proceedings of the National Academy of Sciences*, *109*(35), 14046–14051. https://doi.org/10.1073/pnas.1212381109

Belanger, C. L., Sharon, Du, J., Payne, C. R., & Mix, A. C. (2020). North Pacific deep-sea ecosystem responses reflect post-glacial switch to pulsed export productivity, deoxygenation, and destratification. *Deep Sea Research Part I: Oceanographic Research Papers*, *164*, 103341. https://doi.org/10.1016/j.dsr.2020.103341

Berelson, W. M. (1991). The flushing of two deep-sea basins, southern California borderland. *Limnology and Oceanography*, *36*(6), 1150–1166. https://doi.org/10.4319/lo.1991.36.6.1150

Berelson, W. M., & Stott, L. D. (2003). Productivity and organic carbon rain to the California margin seafloor: Modern and paleoceanographic perspectives. *Paleoceanography*, *18*(1), 2-1-2–15. https://doi.org/10.1029/2001PA000672

Bernhard, J. M., & Gupta, B. K. S. (1999). Foraminifera of oxygen-depleted environments. In *Modern foraminifera* (pp. 201–216). Springer.

Bograd, S. J., Buil, M. P., Lorenzo, E. D., Castro, C. G., Schroeder, I. D., Goericke, R., Anderson, C. R., Benitez-Nelson, C., & Whitney, F. A. (2015). Changes in source waters to the Southern California Bight. *Deep Sea Research Part II: Topical Studies in Oceanography*, *112*, 42–52. https://doi.org/10.1016/j.dsr2.2014.04.009

Bograd, S. J., Castro, C. G., Di Lorenzo, E., Palacios, D. M., Bailey, H., Gilly, W., & Chavez, F. P. (2008). Oxygen declines and the shoaling of the hypoxic boundary in the California Current. *Geophysical Research Letters*, *35*(12). https://doi.org/Artn L12607 10.1029/2008gl034185

736 Bograd, S. J., Checkley, D. A., & Wooster, W. S. (2003). CalCOFI: A half century of physical, chemical,
737 and biological research in the California Current System. *Deep Sea Research Part II: Topical*
738 *Studies in Oceanography*, *50*(14), 2349–2353. https://doi.org/10.1016/S0967-0645(03)00122-X
739 Bograd, S. J., & Lynn, R. J. (2003). Long-term variability in the Southern California Current System.
740 *Deep Sea Research Part II: Topical Studies in Oceanography*, *50*(14), 2355–2370.
741 https://doi.org/10.1016/S0967-0645(03)00131-0
742 Bograd, S. J., Schroeder, I. D., & Jacox, M. G. (2019). A water mass history of the Southern California
743 current system. *Geophysical Research Letters*, *46*(12), 6690–6698.
744 https://doi.org/10.1029/2019GL082685
745 Breitburg, D., Levin, L. A., Oschlies, A., Gregoire, M., Chavez, F. P., Conley, D. J., Garcon, V., Gilbert,
746 D., Gutierrez, D., Isensee, K., Jacinto, G. S., Limburg, K. E., Montes, I., Naqvi, S. W. A., Pitcher,
747 G. C., Rabalais, N. N., Roman, M. R., Rose, K. A., Seibel, B. A., … Zhang, J. (2018). Declining
748 oxygen in the global ocean and coastal waters. *Science*, *359*(6371), 46-+.
749 https://doi.org/10.1126/science.aam7240
750 Cannariato, K. G., & Kennett, J. P. (1999). Climatically related millennial-scale fluctuations in strength of
751 California margin oxygen-minimum zone during the past 60 k.y. *Geology*, *27*(11), 975–978.
752 https://doi.org/Doi 10.1130/0091-7613(1999)027<0975:Crmsfi>2.3.Co;2
753 Cardich, J., Gutiérrez, D., Romero, D., Pérez, A., Quipúzcoa, L., Marquina, R., Yupanqui, W., Solís, J.,
754 Carhuapoma, W., Sifeddine, A., & Rathburn, A. (2015). Calcareous benthic foraminifera from
755 the upper central Peruvian margin: Control of the assemblage by pore water redox and
756 sedimentary organic matter. *Marine Ecology Progress Series*, *535*, 63–87.
757 https://doi.org/10.3354/meps11409
758 Cardich, J., Sifeddine, A., Salvatteci, R., Romero, D., Briceño-Zuluaga, F., Graco, M., Anculle, T.,
759 Almeida, C., & Gutiérrez, D. (2019). Multidecadal Changes in Marine Subsurface Oxygenation
760 Off Central Peru During the Last ca. 170 Years. *Frontiers in Marine Science*, *6*.
761 https://doi.org/10.3389/fmars.2019.00270
762 Caulle, C., Koho, K. A., Mojtahid, M., Reichart, G. J., & Jorissen, F. J. (2014). Live (Rose Bengal
763 stained) foraminiferal faunas from the northern Arabian Sea: Faunal succession within and below
764 the OMZ. *Biogeosciences*, *11*(4), 1155–1175. https://doi.org/10.5194/bg-11-1155-2014
765 Checkley, D. M., & Barth, J. A. (2009). Patterns and processes in the California Current System.
766 *Progress in Oceanography*, *83*(1–4), 49–64. https://doi.org/10.1016/j.pocean.2009.07.028
767 Christensen, C. J., Gorsline, D. S., Hammond, D. E., & Lund, S. P. (1994). Non-annual laminations and
768 expansion of anoxic basin-floor conditions in Santa Monica Basin, California Borderland, over
769 the past four centuries. *Marine Geology*, *116*(3–4), 399–418.

De, S., & Gupta, A. K. (2010). Deep-sea faunal provinces and their inferred environments in the Indian Ocean based on distribution of Recent benthic foraminifera. *Palaeogeography, Palaeoclimatology, Palaeoecology*, *291*(3), 429–442. https://doi.org/10.1016/j.palaeo.2010.03.012

Erdem, Z., Schönfeld, J., Rathburn, A. E., Perez, M.-E., Cardich, J., & Glock, N. (2019). Bottom-water deoxygenation at the Peruvian Margin during the last deglaciation recorded by benthic foraminifera. *Biogeosciences Discussions*. https://orcid.org/0000-0002-5509-8733

Evans, N., Schroeder, I. D., Buil, M. P., Jacox, M. G., & Bograd, S. J. (2020). Drivers of Subsurface Deoxygenation in the Southern California Current System. *Geophysical Research Letters*, *47*(21), e2020GL089274. https://doi.org/10.1029/2020GL089274

Fenton, I. S., Baranowski, U., Boscolo-Galazzo, F., Cheales, H., Fox, L., King, D. J., Larkin, C., Latas, M., Liebrand, D., Miller, C. G., Nilsson-Kerr, K., Piga, E., Pugh, H., Remmelzwaal, S., Roseby, Z. A., Smith, Y. M., Stukins, S., Taylor, B., Woodhouse, A., … Purvis, A. (2018). Factors affecting consistency and accuracy in identifying modern macroperforate planktonic foraminifera. *Journal of Micropalaeontology*, *37*(2), 431–443. https://doi.org/10.5194/jm-37-431-2018

Fisler, J., & Hendy, I. L. (2008). California Current System response to late Holocene climate cooling in southern California. *Geophysical Research Letters*, *35*(9). https://doi.org/Artn L09702 10.1029/2008gl033902

Fleming, K., Johnston, P., Zwartz, D., Yokoyama, Y., Lambeck, K., & Chappell, J. (1998). Refining the eustatic sea-level curve since the Last Glacial Maximum using far- and intermediate-field sites. *Earth and Planetary Science Letters*, *163*(1), 327–342. https://doi.org/10.1016/S0012-821X(98)00198-8

Forcino, F. L., Leighton, L. R., Twerdy, P., & Cahill, J. F. (2015). Reexamining Sample Size Requirements for Multivariate, Abundance-Based Community Research: When Resources are Limited, the Research Does Not Have to Be. *PLOS ONE*, *10*(6), e0128379. https://doi.org/10.1371/journal.pone.0128379

France, S. C. (1994). Genetic population structure and gene flow among deep-sea amphipods,Abyssorchomene spp., from six California Continental Borderland basins. *Marine Biology*, *118*(1), 67–77. https://doi.org/10.1007/BF00699220

Gardner, J. V., Heusser, L. E., Quinterno, P. J., Stone, S. M., Barron, J. A., & Poore, R. Z. (1988). Clear Lake record vs. The adjacent marine record; A correlation of their past 20,000 years of paleoclimatic and paleoceanographic responses. In *Geological Society of America Special Papers* (Vol. 214, pp. 171–182). Geological Society of America. https://doi.org/10.1130/SPE214-p171

803 Helly, J. J., & Levin, L. A. (2004). Global distribution of naturally occurring marine hypoxia on
804 continental margins. *Deep-Sea Research Part I-Oceanographic Research Papers*, *51*(9), 1159–
805 1168. https://doi.org/10.1016/j.dsr.2004.03.009
806 Ingram, B. L., & Southon, J. R. (1996). Reservoir ages in eastern Pacific coastal and estuarine waters.
807 *Radiocarbon*, *38*(3), 573–582.
808 Jaccard, S. L., Galbraith, E. D., Frolicher, T. L., & Gruber, N. (2014). Ocean (De)Oxygenation across the
809 Last Deglaciation Insights for the Future. *Oceanography*, *27*(1), 26–35.
810 Kaiho, K. (1994). Benthic Foraminiferal Dissolved-Oxygen Index and Dissolved-Oxygen Levels in the
811 Modern Ocean. *Geology*, *22*(8), 719–722. https://doi.org/Doi 10.1130/0091-
812 7613(1994)022<0719:Bfdoia>2.3.Co;2
813 Kaiho, K. (1999). Effect of organic carbon flux and dissolved oxygen on the benthic foraminiferal oxygen
814 index (BFOI). *Marine Micropaleontology*, *37*(1), 67–76. https://doi.org/Doi 10.1016/S0377-
815 8398(99)00008-0
816 Keating-Bitonti, C. R., & Payne, J. L. (2016). Physicochemical controls on biogeographic variation of
817 benthic foraminiferal test size and shape. *Paleobiology*, *42*(4), 595–611.
818 Keating-Bitonti, C. R., & Payne, J. L. (2017). Ecophenotypic responses of benthic foraminifera to oxygen
819 availability along an oxygen gradient in the California Borderland. *Marine Ecology*, *38*(3).
820 Keating-Bitonti, C. R., & Payne, J. L. (2018). Environmental influence on growth history in marine
821 benthic foraminifera. *Paleobiology*, *44*(4), 736–757. https://doi.org/10.1017/pab.2018.19
822 Kemp, A. C., Wright, A. J., & Cahill, N. (2020). Enough is Enough, or More is More? Testing the
823 Influence of Foraminiferal Count Size on Reconstructions of Paleo-Marsh Elevation. *Journal of*
824 *Foraminiferal Research*, *50*(3), 266–278. https://doi.org/10.2113/gsjfr.50.3.266
825 Levin, L. A. (2003). Oxygen minimum zone benthos: Adaptation and community response to hypoxia.
826 *Oceanography and Marine Biology, Vol 41*, *41*, 1–45.
827 Levin, L. A., Ekau, W., Gooday, A. J., Jorissen, F., Middelburg, J. J., Naqvi, S. W. A., Neira, C.,
828 Rabalais, N. N., & Zhang, J. (2009). Effects of natural and human-induced hypoxia on coastal
829 benthos. *Biogeosciences*, *6*(10), 2063–2098. https://doi.org/10.5194/bg-6-2063-2009
830 McGann, M. (2011). Paleoceanographic changes on the Farallon Escarpment off central California during
831 the last 16,000 years. *Quaternary International*, *235*, 26–39.
832 https://doi.org/10.1016/j.quaint.2010.09.005
833 Moffitt, S. E., Hill, T. M., Ohkushi, K., Kennett, J. P., & Behl, R. J. (2014). Vertical oxygen minimum
834 zone oscillations since 20 ka in Santa Barbara Basin: A benthic foraminiferal community
835 perspective. *Paleoceanography*, *29*(1), 44–57. https://doi.org/10.1002/2013pa002483

836 Moffitt, S. E., Hill, T. M., Roopnarine, P. D., & Kennett, J. P. (2015). Response of seafloor ecosystems to
837 abrupt global climate change. *Proceedings of the National Academy of Sciences of the United*
838 *States of America*, *112*(15), 4684–4689. https://doi.org/10.1073/pnas.1417130112
839 Murgese, D. S., & De Deckker, P. (2005). The distribution of deep-sea benthic foraminifera in core tops
840 from the eastern Indian Ocean. *Marine Micropaleontology*, *56*(1), 25–49.
841 https://doi.org/10.1016/j.marmicro.2005.03.005
842 Myhre, S. E., Kroeker, K. J., Hill, T. M., Roopnarine, P., & Kennett, J. P. (2017). Community benthic
843 paleoecology from high-resolution climate records: Mollusca and foraminifera in post-glacial
844 environments of the California margin. *Quaternary Science Reviews*, *155*, 179–197.
845 https://doi.org/10.1016/j.quascirev.2016.11.009
846 Ohkushi, K., Kennett, J. P., Zeleski, C. M., Moffitt, S. E., Hill, T. M., Robert, C., Beaufort, L., & Behl, R.
847 J. (2013). Quantified intermediate water oxygenation history of the NE Pacific: A new benthic
848 foraminiferal record from Santa Barbara basin. *Paleoceanography*, *28*(3), 453–467.
849 https://doi.org/10.1002/palo.20043
850 Oksanen, J., Blanchet, F. G., Kindt, R., Legendre, P., Minchin, P. R., O'hara, R. B., Simpson, G. L.,
851 Solymos, P., Stevens, M. H. H., & Wagner, H. (2013). Package 'vegan.' *Community Ecology*
852 *Package, Version*, *2*(9).
853 Oschlies, A., Brandt, P., Stramma, L., & Schmidtko, S. (2018). Drivers and mechanisms of ocean
854 deoxygenation. *Nature Geoscience*, *11*(7), 467–473. https://doi.org/10.1038/s41561-018-0152-2
855 Palmer, H. M., Hill, T. M., Roopnarine, P. D., Myhre, S. E., Reyes, K. R., & Donnenfield, J. T. (2020).
856 Southern California margin benthic foraminiferal assemblages record recent centennial-scale
857 changes in oxygen minimum zone. *Biogeosciences*, *17*(11), 2923–2937.
858 https://doi.org/10.5194/bg-17-2923-2020
859 Praetorius, S. K., Mix, A. C., Walczak, M. H., Wolhowe, M. D., Addison, J. A., & Prahl, F. G. (2015).
860 North Pacific deglacial hypoxic events linked to abrupt ocean warming. *Nature*, *527*(7578), 362-
861 +. https://doi.org/10.1038/nature15753
862 Rathburn, A. E., Willingham, J., Ziebis, W., Burkett, A. M., & Corliss, B. H. (2018). A New biological
863 proxy for deep-sea paleo-oxygen: Pores of epifaunal benthic foraminifera. *Scientific Reports*,
864 *8*(1), 9456. https://doi.org/10.1038/s41598-018-27793-4
865 Roark, E. B., Ingram, B. L., Southon, J., & Kennett, J. P. (2003). Holocene foraminiferal radiocarbon
866 record of paleocirculation in the Santa Barbara Basin. *Geology*, *31*(4), 379–382.
867 https://doi.org/Doi 10.1130/0091-7613(2003)031<0379:Hfrrop>2.0.Co;2

868 Schimmelmann, A., Hendy, I. L., Dunn, L., Pak, D. K., & Lange, C. B. (2013). Revised similar to 2000-
869 year chronostratigraphy of partially varved marine sediment in Santa Barbara Basin, California.
870 *Gff*, *135*(3–4), 258–264. https://doi.org/10.1080/11035897.2013.773066
871 Schmidtko, S., Stramma, L., & Visbeck, M. (2017). Decline in global oceanic oxygen content during the
872 past five decades. *Nature*, *542*(7641), 335-+. https://doi.org/10.1038/nature21399
873 Sharon, Belanger, C., Du, J., & Mix, A. (2021). Reconstructing Paleo-oxygenation for the Last 54,000
874 Years in the Gulf of Alaska Using Cross-validated Benthic Foraminiferal and Geochemical
875 Records. *Paleoceanography and Paleoclimatology*, *36*(2), e2020PA003986.
876 https://doi.org/10.1029/2020PA003986
877 Stott, L. D., Neumann, M., & Hammond, D. (2000). Intermediate water ventilation on the northeastern
878 Pacific margin during the late Pleistocene inferred from benthic foraminiferal delta C-13.
879 *Paleoceanography*, *15*(2), 161–169. https://doi.org/Doi 10.1029/1999pa000375
880 Stramma, L., Johnson, G. C., Firing, E., & Schmidtko, S. (2010). Eastern Pacific oxygen minimum zones:
881 Supply paths and multidecadal changes. *Journal of Geophysical Research: Oceans*, *115*(C9).
882 Stramma, L., Schmidtko, S., Levin, L. A., & Johnson, G. C. (2010). Ocean oxygen minima expansions
883 and their biological impacts. *Deep-Sea Research Part I-Oceanographic Research Papers*, *57*(4),
884 587–595. https://doi.org/10.1016/j.dsr.2010.01.005
885 Stuiver, M., & Polach, H. A. (1977). Discussion reporting of 14 C data. *Radiocarbon*, *19*(3), 355–363.
886 Talley, L. D. (1993). Distribution and Formation of North Pacific Intermediate Water. *Journal of Physical*
887 *Oceanography*, *23*(3), 517–537. https://doi.org/10.1175/1520-
888 0485(1993)023<0517:DAFONP>2.0.CO;2
889 Taylor, M. A., Hendy, I. L., & Pak, D. K. (2015). The California Current System as a transmitter of
890 millennial scale climate change on the northeastern Pacific margin from 10 to 50 ka.
891 *Paleoceanography*, *30*(9), 1168–1182. https://doi.org/10.1002/2014pa002738
892 Tetard, M., Licari, L., Tachikawa, K., Ovsepyan, E., & Beaufort, L. (2021). Toward a global calibration
893 for quantifying past oxygenation in oxygen minimum zones using benthic Foraminifera.
894 *Biogeosciences Discussions*, 1–17. https://doi.org/10.5194/bg-2020-482
895 Venturelli, R. A., Rathburn, A., Burkett, A., & Ziebis, W. (2018). Epifaunal Foraminifera in an Infaunal
896 World: Insights Into the Influence of Heterogeneity on the Benthic Ecology of Oxygen-Poor,
897 Deep-Sea Habitats. *Frontiers in Marine Science*, *5*, 344.
898 Wang, Y., Hendy, I. L., & Zhu, J. (2020). Expansion of the Southern California oxygen minimum zone
899 during the early-to mid-Holocene due to reduced ventilation of the Northeast Pacific. *Quaternary*
900 *Science Reviews*, *238*, 106326. https://doi.org/10.1016/j.quascirev.2020.106326
901